OPTICAL TOMOGRAPHY BASED ON A NONLINEAR MODEL THAT HANDLES MULTIPLE SCATTERING

Morteza Hasani Shoreh[1], Alexandre Goy[1], JooWon Lim[1], Ulugbek Kamilov[2], Michael Unser[3], and Demetri Psaltis[1]

[1]Optics Laboratory, École Polytechnique Fédérale de Lausanne (EPFL, Switzerland.
[2]Mitsubishi Electronic Research Laboratories (MERL), Cambridge, MA 02139, USA.
[3]Biomedical Imaging Group, École Polytechnique Fédérale de Lausanne (EPFL), Switzerland.

ABSTRACT

Learning Tomography (LT) is a nonlinear optimization algorithm for computationally imaging three-dimensional (3D) distribution of the refractive index in semi-transparent samples. Since the energy function in LT is generally non-convex, the solution it obtains is not guaranteed to be globally optimal. In this paper, we describe linear and nonlinear tomographic reconstruction methods and compare them numerically. We present a review of the LT and, in addition, we investigate the influence of the initialization and exemplify the effect of regularization on the convergence of the algorithm. In particular, we show that both are essential for high-quality imaging in strongly scattering scenarios.

Index Terms— Optical tomography, digital holography, multiple scattering, computational imaging, nonlinear optimization.

1. INTRODUCTION

Optical inverse scattering has recently received great attention from the scientific community. One of the natural avenues to further improve optical microscopy is to account for the multiple scattering of light as it passes through the sample. This is of particular importance in biological tissues because of the rise of biological applications and the fact that tissues can be strongly scattering. Moreover, the study of dynamical process requires minimally invasive in vivo imaging techniques. Optical tomography (OT) is a non-toxic technique for three-dimensional (3D) imaging of the refractive index distribution in biological samples [1]. The knowledge of the refractive index allows one to characterize the scattering properties of the sample. This has a potential to improve many traditional microscopy methods. For example, one can improve fluorescence microscopy [2] by taking advantage of wavefront correction techniques [3].

Mapping the refractive index of a sample is now conventionally performed using optical diffraction tomography (DT). This technique has been extensively studied in the optics community [4-10]. The initial study [4] was based on the first Born approximation that accounted for single scattering only, which implies a linear relationship between the scattering potential and the scattered field. Such a method is, however, limited to weakly scattering objects. Improvement in reconstruction accuracy was then brought by the Rytov approximation [11, 12]. Both the Rytov and first Born approximations provide direct formulas to solve the inverse scattering problem, i.e., the problem of going from the measurements of the scattered field to a model of the refractive index distribution within the sample. For multiple scattering, the problem becomes nonlinear and there is no known closed-form formula. The natural way of performing inverse scattering is through numerical optimization. Such techniques have been thoroughly investigated in many area of science and has been recently exported to the field of optical tomography [13].

In recent works [14, 15], we introduced learning tomography (LT), a nonlinear optimization method using the beam propagation method (BPM) as a nonlinear forward model. The results showed that it was possible to account for multiple scattering using the BPM. As generally occurs for nonlinear problems, the optimization algorithm may fall in local minima of the energy function. In this paper, we study the influence of two crucial components of LT, the initialization and total variation (TV) regularization, to the convergence of the method. In particular, we numerically compare the constant initialization against the one obtained with Diffraction tomography under Rytov approximation [12]. Additionally, we compare the reconstruction quality with and without TV regularization. Note that unlike the work in [13], our learning tomography approach relies on

digital holography for measuring the complex scattered field and considers sparsity-driven TV regularization.

2. LEARNING TOMOGRPAHY

As other optical tomography methods, LT aims at solving the inverse scattering problem. In this particular case we are interested in recovering the three-dimensional refractive index distribution $n(r)$ of an unknown sample from the measurement of the complex optical field scattered as the sample is illuminated with plane waves at different angles of incidence. This is illustrated in Fig. 1.

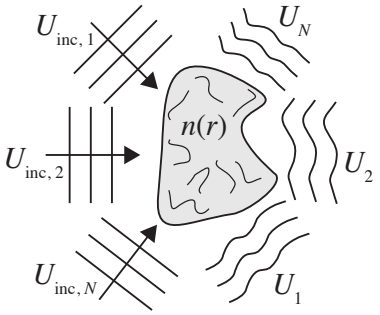

Fig. 1: Principle of the optical tomography. The scattering object is illuminated by N plane waves under different incidence angles. The scattered field U_i is recorded for each incident wave.

The object is described by its scattering potential F defined as: $F(r) = k^2(n(r)^2 - n_0^2)/(4\pi)$, in which n_0 is the refractive index of the background material and k is the wave-vector of the illumination light in the background medium. The scattering of monochromatic coherent light is modeled by the following inhomogeneous Helmholtz equation:

$$\nabla^2 U + k^2 U = -4 \quad F(\mathbf{r})U \,, \tag{1}$$

in which the refractive index is space-dependent. This equation assumes an equivalent integral form, the Lippmann-Schwinger equation:

$$U(\mathbf{r}) = U_{\text{inc}}(\mathbf{r}) + \int F(\mathbf{r}')G(\mathbf{r}-\mathbf{r}')U(\mathbf{r}')d\mathbf{r}' \,, \tag{2}$$

in which U is the total field, U_{inc} the incident field, and G the Green's function of the Helmholtz operator $\nabla^2 + k^2$. It is clear from equations (1) and (2) that the total field, hence he scattered field, are nonlinear function of the scattering potential. As we have shown in previous publications [14, 15], the split-step Fourier beam propagation method (BPM) is an efficient numerical solver for equation (1) [16]. Apart from its speed and numerical stability, the BPM has also been chosen as a forward model because it allows for a fast calculation of the gradient of the error function defined below. The BPM accounts for the nonlinearity of the system and naturally also for multiple scattering.

The main idea of LT is not to find a direct inversion formula for the nonlinear scattering problem, but rather to solve it as an optimization problem.

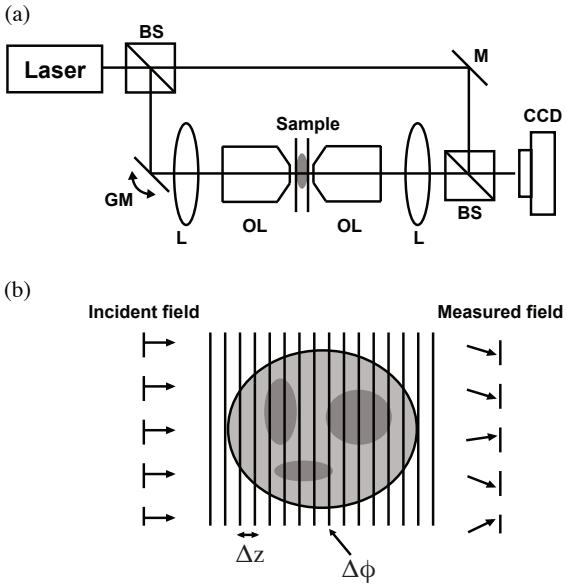

Fig. 2: (a) General experimental setup for optical tomography. A coherent source, such as a laser is used. The structure is that of a Mac-Zehnder interferometer set up for digital holographic measurement (BS = beam splitter, M = mirror). Galvo-mirrors (GM) are placed in the signal beam in order to change the incidence angle of the light on the sample. The sample itself is placed between two microscope objectives (MO). The interferogram is captured on a CCD camera and the complex field is extracted digitally.
(b) Principle of the beam propagation method (BPM). The object is split into N_z slices, separated by a distance Δz along the main propagation direction z. The scattering within the object is represented, at each slice, by a phase mask $\Delta\varphi_z(x, y)$ that accounts for refractive index variations. Between the phase masks, the light is propagated using Fresnel diffraction in a homogeneous medium of refractive index n_0.

We start our optimization with some initial guess for the refractive index. From that guess, we calculate a set of predicted measurements using the BPM and compare the prediction to the actual measurements recorded in the experiment under the same illumination angles. The error is defined as the difference between the prediction and the measurement:

$$\varepsilon(n) = \frac{1}{N}\sum_i \left\| h_i(n) - m_i \right\|^2 , \tag{3}$$

where N is the number of views, m_i is the actual experimental measurement and h_i the BPM operator under illumination angle i. Another significant element of the algorithm, is the use of a regularizing operator at each iteration, as demonstrated in [17]. In particular, we use TV for edge-preserving piecewise-smooth regularization [18]. In addition to TV, we impose lower and upper bounds on the refractive index contrast, depending on the nature of the

object. The regularizer is denoted by R, and the total cost function that we minimize is defined as:

$$J(n) = \varepsilon(n) + \tau R(n), \quad (4)$$

where $\tau > 0$ is a regularization parameter. The estimate of the refractive index is given by

$$\hat{n} = \arg\min_{n} J(n). \quad (5)$$

We carry out the optimization by calculating the gradient [15] of the error ε at each step for gradient-based optimization.

3. IMPORTANCE OF THE INITIAL GUESS

In this section, we detail the methods we use to calculate the initial guess used to initiate the LT algorithm. We compute the tomographic reconstruction from the measurements using the following methods:

Zero initialization

In case of zero initialization, the LT algorithm is started with no object and light is propagated in a homogeneous medium with constant background refractive index n_0. Therefore, at the first iteration of LT, the predicted field by BPM is just the propagation of the incident filed. The residual – the difference between the prediction by BPM and the experimental measurement – is the scattered field itself. The gradient calculated at the first iteration is thus based on the scattered field.

Radon tomography

In this case, diffraction effects are neglected and the light rays are assumed to propagate along straight lines. Each ray accumulates a phase proportional to the optical path it encounters through the object. The object is reconstructed slice by slice, each slice being taken perpendicularly to the X axis. The incident light beam axis stays perpendicular to the X axis and is rotated along it. For each angle, the detected data is mapped into a sinogram that can be readily inverted using the inverse Radon transform [19] at the end of acquisition.

Diffraction tomography with Born and Rytov approximations

Under the assumption of weak scattering, the scattered field is much smaller than the incident field. In this case, the total field within the integrand of equation (2) can be replaced by the incident field:

$$U_s(\mathbf{r}) = \int_V F(\mathbf{r}')G(\mathbf{r}-\mathbf{r}')U_{\text{inc}}(\mathbf{r}')d\mathbf{r}' \quad (6)$$

This is widely known as the first Born approximation. The consequence of this substitution is that the scattered field can be evaluated directly without solving any nonlinear equation. The scattered field becomes thus a linear function of the scattering potential. Emil Wolf [5] derived a direct formula to solve the inverse scattering problem under the first Born approximation. This formula, that we may call the Wolf transform is the foundation of diffraction tomography.

A variation of this method is obtained by using the first order Rytov approximation. We first perform a change of variable: $U(\mathbf{r}) = e^{\phi_S(\mathbf{r})+\phi_{\text{inc}}(\mathbf{r})}$ and $U_{\text{inc}}(\mathbf{r}) = e^{\phi_{\text{inc}}(\mathbf{r})}$. The following equation can be derived [6]:

$$\phi_s(\mathbf{r})U_{\text{inc}}(\mathbf{r}) = \int_V F(\mathbf{r}')G(\mathbf{r}-\mathbf{r}')U_{\text{inc}}(\mathbf{r}')d\mathbf{r}' \quad (7)$$

For both approximations, the scattered field that is measured is related to the Fourier transform of the scattering potential F object. The measurements are mapped onto the surface of the corresponding Ewald sphere in the Fourier domain. For a given illumination angle, the Ewald sphere is defined by $\left(k-k_x^i\right)^2+\left(k-k_y^i\right)^2+\left(k-k_z^i\right)^2 = k^2 = \left(\frac{2\ n_0}{\ }\right)^2$, where $\mathbf{k}^i = \left(k_x^i, k_y^i, k_z^i\right)$ is the propagation direction of the incident field, n_0 is the refractive index of the medium and λ is the wavelength in free space. Once the measurements have been projected, we recover F by taking the inverse Fourier transform of the union of all Ewald spheres properly filled with the corresponding measurements.

4. RESULTS AND DISCUSSION

We carried out scattering simulation on a homogeneous 15-micron sphere embedded in a homogeneous material of refractive index n_0. We study two cases by tuning the refractive index of the object: in the first case, shown in the left part of Fig. 3, the total optical phase shift induced the object is less than a period, i.e. less than 2π. In the second case, shown on the right part of Fig. 3, the phase shift is larger than 2π. The linear algorithm used to produce the initial guess, in the first row of Fig.3 is diffraction tomography under Rytov approximation. This reconstruction suffers from severe artifacts that are suppressed by the regularized LT optimization.

The result of the simulation as whether LT can approach the best solution, strongly depends on the total phase shift. For weak phase shifts, the algorithm can converge with the help of regularization and proper initialization. For larger phase shifts, the algorithm fails to converge even with regularization and hard constraint on the upper and lower bounds of the refractive index. We interpret this phenomenon as the expression of the phase wrapping. Phase wrapping induces an ambiguity in the measurements that correspond to deep local minima in the cost function.

In Fig. 4, we show reconstruction obtained with the LT algorithm from experimental measurements on a 5 micron polystyrene beads immersed in oil. We show the

reconstructions for four different initial guesses: constant refractive index, Radon transform, and diffraction tomography with Born and Rytov approximation. The experimental results essentially corroborate the simulations in the case of constant and Rytov approximation initial guesses. The total phase delay across the beads is above 2π, and the meansurement have been unwrapped accordingly.

Our simulation and experimental results also indicate that TV regularization is essential for obtaining the best possible LT reconstruction. In particular, for a weekly scattering object (left), LT with TV is able to reconstruct the bead even from zero initialization. The quality of the reconstruction is further boosted by using the diffraction tomography initialization. On the other hand, for strongly scattering scenarios (right), TV regularization without DT initialization yields poor results. This highlights the fact that TV must be supplemented with a good initializer for obtaining the best results in strongly scattering scenarios.

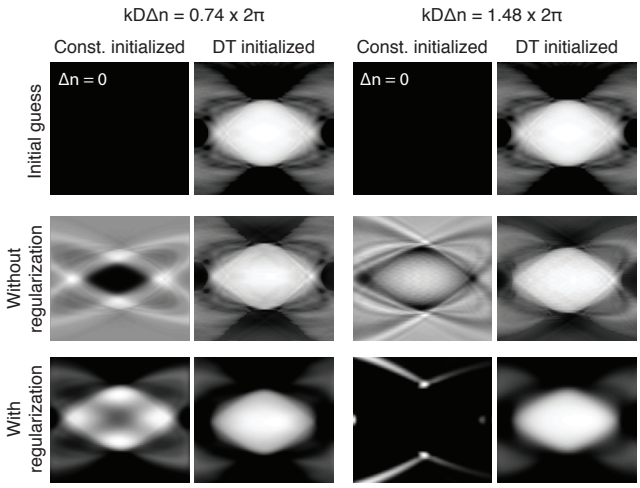

Fig. 3: Simulation illustrating the importance of the initial guess on the performance of the LT algorithm. The object is a 15 micron sphere in a n = 1.5 refractive index background, illuminated at a wavelength of 532nm. All images are YZ cross sections. The gray scale on each figure is the same and is linear from black (n = 1.5) to white (n = 1.55). Left two columns: The object has a refractive index contrast of Δn = 0.026, which leads to a total phase shift of 0.76 x 2π. The top row shows the initial guesses, constant zero on the left and Diffraction Tomography with Rytov approximation on the right. The second row shows the outcome of LT with no regularization (20 iterations) when initiated with the corresponding initial guesses above. The third shows the outcome of LT with TV regularization at each step, starting from the same corresponding intitial guesses. Right two columns: simulations corresponding to the right two columns but with an object contrast of Δn = 0.052, which leads to a total phase shift of 1.48 x 2π.

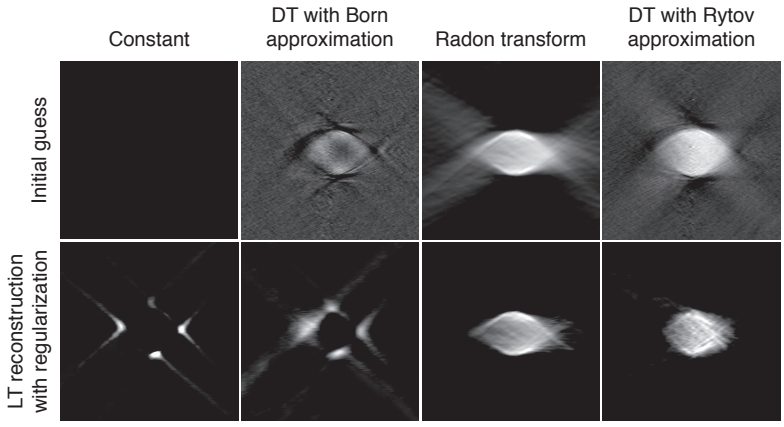

Fig. 4: Experimental reconstruction obtained with the LT algorithm (second row) from four different initial guesses (first row, from left to right): constant refractive index set to n_0 = 1.52, diffraction tomography reconstruction under Born approximation, reconstruction using Radon transform, and diffraction tomography reconstruction under Born approximation.

5. REFERENCES

[1] S. R. Arridge, "Optical tomography in medical imaging," *Inv. Prob.*, vol. 15, no. 2, pp. R41, 1999.

[2] D. A. Agard, Y. Hiraoka, P. Shaw, and J. W. Sedat, "Fluorescence microscopy in three dimensions," *Meth. in Cell Bio.*, vol. 30, pp. 35–377,1989.

[3] A. Jesacher, A. Schwaighofer, S. Fürhapter, C. Maurer, S. Bernet, and M. Ritsch-Marte, "Wavefront correction of spatial light modulators using an optical vortex image," *Opt. Exp.*, vol. 15, no. 9, pp. 5801–5808, 2007.

[4] E. Wolf, "Three-dimensional structure determination of semi-transparent objects from holographic data," *Opt. Comm.*, vol. 1, pp. 153–156, 1969.

[5] V. Lauer, "New approach to optical diffraction tomography yielding a vector equation of diffraction tomography and a novel tomographic microscope," *Jour. of Mic.*, vol. 205, pp. 165–176, 2002.

[6] F. Charrière, A. Marian, F. Montfort, J. Kuehn, T. Colomb, E. Cuche, P. Marquet, and C. Depeursinge, "Cell refractive index tomography by digital holographic microscopy," *Opt. Lett.*, vol. 31, no. 2, pp. 178–180, 2006.

[7] W. Choi, C. Fang-Yen, K. Badizadegan, S. Oh, N. Lue, R. R. Dasari, and M. S. Feld, "Tomographic phase microscopy," *Nat. Meth.*, vol. 4 , pp. 717–719, 2007.

[8] W. Choi, C. Fang-Yen, K. Badizadegan, R. R. Dasari, and M. S. Feld, "Extended depth of focus in tomographic phase microscopy using a propagation algorithm," *Opt. Lett.*, vol. 33, no. 2, pp. 171–173, 2008.

[9] Y. Sung, W. Choi, Christopher Fang-Yen, K. Badizadegan, R. R. Dasari, and M. S. Feld. "Optical diffraction tomography for high resolution live cell imaging," *Opt. Exp.*, vol. 17, no. 1, pp. 266–277, 2009.

[10] Y. Cotte, F. Toy, P. Jourdain, N. Pavillon, D. Boss, P. Magistretti, P. Marquet, and C. Depeursinge, "Marker-free phase nanoscopy," *Nat. Phot.*, vol. 7, no. 2, pp. 113–117, 2013.

[11] V. I. Tatarski, *Wave Propagation in a Turbulent Medium*, Chapt. 7, McGraw-Hill, 1961.

[12] A. J. Devaney, "Inverse-scattering theory within the Rytov approximation," *Opt. Lett.*, vol. 6, no. 8, pp. 374–376, 1981.

[13] L. Tian and L. Waller, "3D intensity and phase imaging from light field measurements in an LED array microscope," *Optica*, vol. 2, no. 2, pp. 104–111, 2015.

[14] U. S. Kamilov, I. N. Papadopoulos, M. H. Shoreh, A. Goy, C. Vonesch, M. Unser, and D. Psaltis, "Learning approach to optical tomography," *Optica*, vol. 2, pp. 517–522, 2015.

[15] U. Kamilov, I. Papadopoulos, M. H. Shoreh, A. Goy, C. Vonesch, M. Unser, and D. Psaltis, "Optical tomographic image reconstruction based on beam propagation and sparse regularization," *IEEE Trans. on Comp. Imag.*, vol. 2, no. 1, pp. 59–70, 2016.

[16] J. V. Roey, J. V. Donk, and P. E. Lagasse, "Beam-propagation method: analysis and assessment," *J. Opt. Soc. Amer. A*, vol. 71, no. 7, pp. 803–810, 1981.

[17] Y. Sung and R. R. Dasari, "Deterministic regularization of three dimensional optical diffraction tomography," *J. Opt. Soc. Amer. A*, vol. 28, no. 8, pp. 1554–1561, 2011.

[18] L. I. Rudin, S. Osher, and E. Fatemi, "Nonlinear total variation based noise removal algorithms," *Physica D*, vol. 60, pp. pp. 259–268, 1992.

[19] J. Radon, "Uber die Bestimmung von Funktionen durch ihre Integralwerte längs gewisser Mannigfaltigkeiten," *Ber. der Sachs. Akad. der Wiss.*, vol. 69, pp. 262–277, 1917.